nature geoscience

Perspective

https://doi.org/10.1038/s41561-025-01743-y

Earth's silicate weathering continuum

Received: 18 December 2023

Accepted: 16 June 2025

Published online: 7 August 2025

Check for updates

Gerrit Trapp-Müller[1] ✉, Jeremy Caves Rugenstein[2], Daniel J. Conley[3], Sonja Geilert[1], Mathilde Hagens[4], Wei-Li Hong[5], Catherine Jeandel[6], Jack Longman[7], Paul R. D. Mason[1], Jack J. Middelburg[1], Kitty L. Milliken[8], Alexis Navarre-Sitchler[9], Noah J. Planavsky[10], Gert-Jan Reichart[1,11], Caroline P. Slomp[12], Appy Sluijs[1], Douwe J. J. van Hinsbergen[1] & Xu Y. Zhang[1]

Chemical weathering of silicate rocks redistributes major, minor and trace elements through coupled dissolution–precipitation reactions. These weathering processes drive shifts in ocean acid–base chemistry, modulating atmospheric carbon dioxide levels and providing a stabilizing feedback in the carbon cycle. Silicate weathering occurs in both terrestrial and marine environments, releasing ('forward') or consuming alkalinity ('reverse'), but these have largely been perceived as independent and studied in isolation. However, weathering products are transported downstream across terrestrial and to marine environments, suggesting a dynamic coupling of these weathering processes across scales. Here we propose that the Earth's silicate weathering occurs along a continuum linking mountains to the deepest sedimentary environments and forward to reverse weathering. In this framework, the magnitude and direction of a local weathering flux depends on the materials' origin, weathering–erosion history and environmental conditions. Consequently, global silicate weathering fluxes and the long-term carbon cycle feedback may be governed by the dynamic interplay of various environments along the silicate weathering continuum.

Chemical silicate weathering (CSW) is the re-equilibration of silicate materials with aqueous environments by coupled dissolution and precipitation reactions[1,2]. CSW redistributes chemical elements amongst Earth's solid and fluid reservoirs in dependence of silicate composition and environmental conditions (Box 1, Fig. 1 and Supplementary Fig. 1), affecting global biogeochemistry and long-term climate[3,4]. In turn, climate affects CSW (on land) via hydrology, biology and temperature, giving rise to a stabilizing carbon cycle feedback[5]. Here, we link old and new observations and theories to derive a comprehensible and mechanistically plausible concept that articulates the systematic variability and continuity of CSW and helps elucidate its enigmatic role in the carbon cycle and Earth system. Relationships and possible covariation with other carbon cycle processes, related to organic matter, carbonate and sulfide minerals[5–7], are briefly discussed.

Traditionally, CSW fluxes are ascribed to terrestrial environments and are quantified regionally or globally by upscaling freshwater solute measurements[8], often omitting submarine groundwater discharge[9]. Terrestrial CSW typically transforms CO_2 into HCO_3^- ('forward' weathering) at rates and efficiencies that depend on lithology, environment and reaction kinetics (Box 1)[10,11]. However, solid weathering

[1]Utrecht University, Utrecht, The Netherlands. [2]Department of Geosciences, Colorado State University, Fort Collins, CO, USA. [3]Department of Geology, Lund University, Lund, Sweden. [4]Soil Chemistry, Wageningen University & Research, Wageningen, The Netherlands. [5]Department of Geological Sciences, Stockholm University, Stockholm, Sweden. [6]LEGOS (CNRS, UT3, IRD, CNES, Université de Toulouse), Observatoire Midi-Pyrénées, Toulouse, France. [7]School of Geography and Environmental Sciences, Northumbria University, Newcastle-Upon-Tyne, UK. [8]Bureau of Economic Geology, University of Texas at Austin, Austin, TX, USA. [9]Geology and Geological Engineering, Colorado School of Mines, Golden, CO, USA. [10]Yale University, New Haven, CT, USA. [11]Department of Ocean Systems, NIOZ, Netherlands Institute for Sea Research, Texel, The Netherlands. [12]Radboud University Nijmegen, Nijmegen, The Netherlands. ✉e-mail: g.muller@uu.nl

https://doi.org/10.1038/s41561-025-01743-y

BOX 1

Silicate weathering balances and the carbon cycle

CSW releases and consumes charged and uncharged molecules through coupled dissolution–precipitation reactions. The charge mismatch is usually compensated by carbonic acid buffering, that is, CO_2–HCO_3^- conversion, so the carbon cycle impact of CSW is quantified via changes in alkalinity (ΔAlk, mol yr^{-1})[60], with ΔAlk > 0 termed forward and ΔAlk < 0 termed reverse weathering. Because reaction balances depend on reactants, environmental conditions and precipitates, the biogeochemical impacts of weathering vary across the weathering continuum, particularly between terrestrial and marine weathering environments.

To quantify this variability, we developed a Monte Carlo reaction balance model (figure in this box and Supplementary Note 1), which we applied to two scenarios of crustal weathering on land (granodiorite–granite and basalt) and to two in continental and mafic–volcanogenic marine sediments (Supplementary Table 1 and Supplementary Data 1). We imposed 10^6 pseudo-randomized (Latin hypercube sampling), literature-constrained reactant and product compositions, and weathering congruencies (10–90% Si reprecipitation), to solve for CSW-related solute and gross alkalinity (Alk_S) fluxes using mass and charge balances. Moreover, iron cycling and $Al(OH)_3$ reactions are included, retaining low-solubility elements (Al, Fe) in the solid phase, so that net alkalinity (Alk_N) fluxes reflect major cation fluxes.

There are systematic differences between continental and basaltic crust weathering on land and marine sediment weathering. Net forward weathering of granitic–granodioritic and basaltic rocks on land provides a net release of major cations and Si, and produces cation-depleted silicates and Al–Fe hydroxides (panels a–c in the figure in this box). In the crustal weathering scenarios, Alk_N is largely governed by reactant composition, increasing with mafic

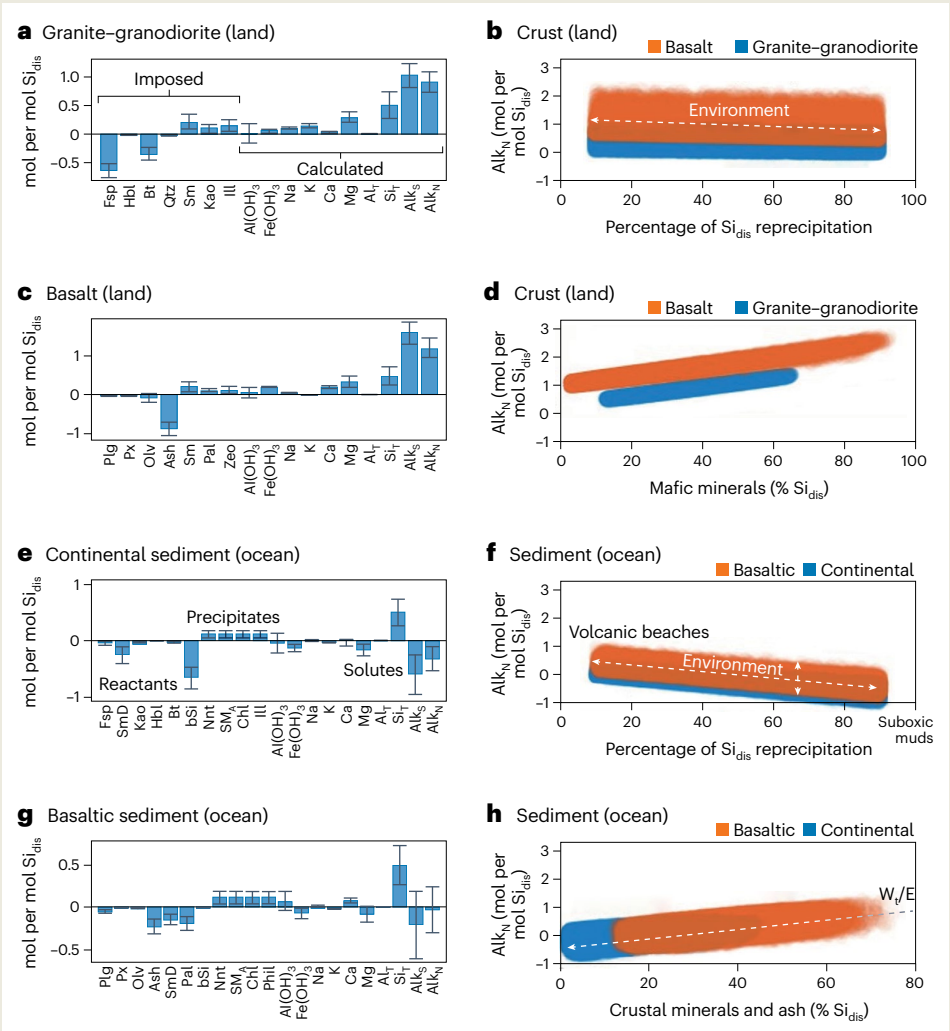

Box Fig. 1 | a,**c**,**e**,**g**, Median and s.d. of 10^5 weathering balances for weathering of granodiorite (**a**) and basalt (**c**) on land, and of continental (**e**) and basaltic (**g**) river particles, including silicate-related alkalinity (AlkS) and net alkalinity (AlkN). **b**,**d**,**f**,**h**, Influences of reactant composition (**d**,**h**) and congruency (reprecipitated Si fraction Si_{dis}, **b**,**f**) on Alk_N. 'Crustal minerals' in **h** exclude quartz for simplicity. Silicates included in the model are feldspar (Fsp), hornblende (Hbl), biotite (Bt), smectite (Sm), kaolinite (Kao), illite (Ill), plagioclase (Plg), pyroxene (Px), olivine (Olv), ash (basaltic), palagonite (Pal), zeolite (Zeo, chabazite), detrital smectite (SmD), biogenic silica (bSi), nontronite (Nnt), authigenic Mg smectite (Sm_A), chlorite (Chl) and phillipsite (Phil).

(continued from previous page)
mineral content, cation/Si and Si/Al ratios from felsic to mafic rocks (panel d in the figure in this box). This implies a stronger negative carbon cycle feedback of basalt compared with granite weathering, consistent with inferences from riverine solute concentrations[11] and thermodynamic weathering models. Thus, lithology (and unconsolidated sedimentary covers) exert a dominant influence on weathering balances and carbon cycle impacts, which is consistent with regional and global-scale models[8,10,39].

In marine sediments, differences between basaltic and continental-rock-derived materials diminish and weathering balances tend towards alkalinity consumption, that is, reverse weathering (panels e–g in the figure in this box). Alk_N is more sensitive to weathering congruency, and strongly moderated by dissimilatory iron sources in reverse scenarios (panels e,g in the figure in this box). These effects largely arise from increasing contributions of cation-poor, terrestrial weathering products and biogenic silica, and from the higher cation content of many marine product silicates (panels f,h in the figure in this box). Thus, marine sediment weathering balances transition from forward to reverse with increasing ratio of terrestrial weathering to erosion (W_t/E), while basaltic ash and crustal minerals (except cation-free quartz) increase Alk_N. These results are consistent with process-based models and experimental and field constraints[14–17,44], and demonstrate that reactant mixtures and environmental conditions govern how CSW proceeds.

products and residues are exported from the upstream watersheds to be weathered downstream in floodplains[12] and marine surface and subsurface environments[13], generating weathering fluxes that can rival those from headwaters (Fig. 1 and Supplementary Fig. 1). In marine sediments, reaction balances transforming HCO_3^- back into CO_2 ('reverse' weathering) become feasible in addition to forward CSW[14–16]. The characteristics of detrital sediments, largely set by upstream CSW and provenance, govern marine sediment biogeochemistry and CSW balances (Box 1) in concert with sedimentary dynamics and marine biogenic supplies[15–19].

Marine CSW is ubiquitous in terrigenous marine surface sediments[13,17,20] and extends deep into the subsurface of sedimentary basins[21,22] (Fig. 1), but is usually ignored or viewed in isolation from terrestrial CSW in carbon cycle and Earth system models[5,6,23–26]. In addition to marine sediment, oceanic crust is an important locus of marine CSW[27]. Eventually, marine sediment CSW couples to hydrothermal systems and oceanic crust weathering[27]. Incorporating a coupling between terrestrial and marine, crustal and sedimentary CSW into the current concepts of the silicate weathering feedback in the carbon cycle[6,24,25] eventually forces a shift in our understanding of Earth system evolution.

The silicate weathering continuum

At the scale of a molecule to a small grain (nanometres to millimetres), CSW rates and reaction balances depend on the starting material (reactants) and the physical (for example, surface or interface properties, shielding, defect structure) and chemical (for example, saturation, ionic strength, pH) conditions at a particle's reactive interface[2,28]. These interfacial conditions are influenced by nanometre- to millimetre-scale internal feedbacks between dissolution, precipitation, solution chemistry and transport[2,29] and by environmental factors including ambient biogeochemistry, water flow, particle motion and biological activity[1,10,17,30,31]. Despite differences in scales and complexity, such nanometre- to millimetre-scale dynamics appear to determine CSW fluxes at regional to global scales, as reflected in soil shielding, reactive surface availability ('land surface reactivity', 'weatherability') or dependence on hydrodynamics in the terrestrial realm[10,32].

The products and residues of terrestrial CSW are eventually transported downstream, where the rate and nature of solid–fluid re-equilibration vary across environments, and where they are mixed with biogenic components, promoting different reaction balances and carbon cycle impacts (Fig. 1 and the figure in Box 1). For instance, marine CSW commonly involves minerals and solutes that may have been generated by previous terrestrial CSW, millions of years earlier and thousands of kilometres away[20,33]. Corresponding biogeochemical conditions vary with the dynamics of organic matter degradation. It is particularly evident in ocean margin surface sediments that biogeochemical conditions and CSW dynamics are sensitive to the sediment's origin and weathering–erosion history[14,15,17,20].

If the removal of terrestrial silicate weathering (W_t, mass/time) products through erosion (E, mass/time) and/or fluid flow exceed their production rate, reaction kinetics limit catchment-wide weathering fluxes[10,34] and the corresponding river particles will arrive relatively unaltered and cation-rich at the floodplain, coast and/or deeper subsurface sediments (for example, many Himalayan and Arctic rivers[34–36]). Such a low W_t/E eventually facilitates downstream forward CSW in floodplain[12] or marine surface and subsurface sediments[15,18] (Box 1 and Supplementary Fig. 1). Tephra deposition directly supplies fresh, cation-rich and reactive silicates that promote forward weathering balances[19,37]. In contrast, if terrestrial erosion and/or solute export cannot keep pace with local CSW rates, solute release becomes limited by the accessibility of weatherable surfaces at the reaction front[8,34,38] or thermodynamics[39]. Under such conditions of high W_t/E ratios, or if cation-depleted sedimentary rocks dominate the upstream lithology, mainly preweathered and cation-depleted, pedogenic materials are discharged to the corresponding floodplains and coasts (for example, the Amazon basin[40] or lateritic valleys of Hawaii[41]). This eventually decreases subsequent CSW-related alkalinity fluxes in downstream environments[12,16] (Box 1). This downstream coupling of weathering balances is supported by consistent global trends of increasing riverine dissolved cation and weathering fluxes[8], soil clay content and thickness[8,42], cation depletion of river sediments[36], terrigenous mud content on the inner shelves[43] and cation-rich marine authigenic clay occurrences[20,44] with decreasing latitude. Moreover, silica release by terrestrial CSW is largely recycled in relatively pure SiO_2 biominerals that react with detrital and hydrothermal particles to form authigenic clays[20,45] and zeolites[46] in many marine sediments, further promoting reverse CSW (Fig. 1 and Box 1). While W_t/E exerts a first-order control on marine CSW balances, rates and fluxes may become limited by terrigenous reactant supply: for example, in distal deep-sea settings, in protected shallow areas or due to low upstream erosion rates.

The physical and biogeochemical conditions in different sedimentary environments directly affect authigenic mineral assemblages and weathering balances and rates[17]. These conditions are, in turn, largely governed by sedimentary dynamics and reactive particle supplies (organic matter, metal (oxy-)hydroxides)[17,20,47]. Organic matter supply to shallow ocean margin sediments is generally high. Thus, anaerobic conditions prevail and CSW balances are governed by organic matter degradation and biomineral dissolution in these sediments. Suboxic, iron-rich conditions stimulate cation-rich green clay authigenesis (for example, odinite, chlorite, Fe-micas) and reverse weathering, particularly at high W_t/E (refs. 16,20,44). Suboxic conditions are promoted by high metal (oxy-)hydroxide supplies and seasonal reworking at low-latitude river-dominated margins of the present ocean (for example, the Amazon[48] and East China shelves[49]) and occur in the upper centimetres of many surface sediments further offshore[20]. In somewhat deeper and more steadily accumulating sediments, sulfidic and methanic conditions dominate[47], under which CSW products and

https://doi.org/10.1038/s41561-025-01743-y

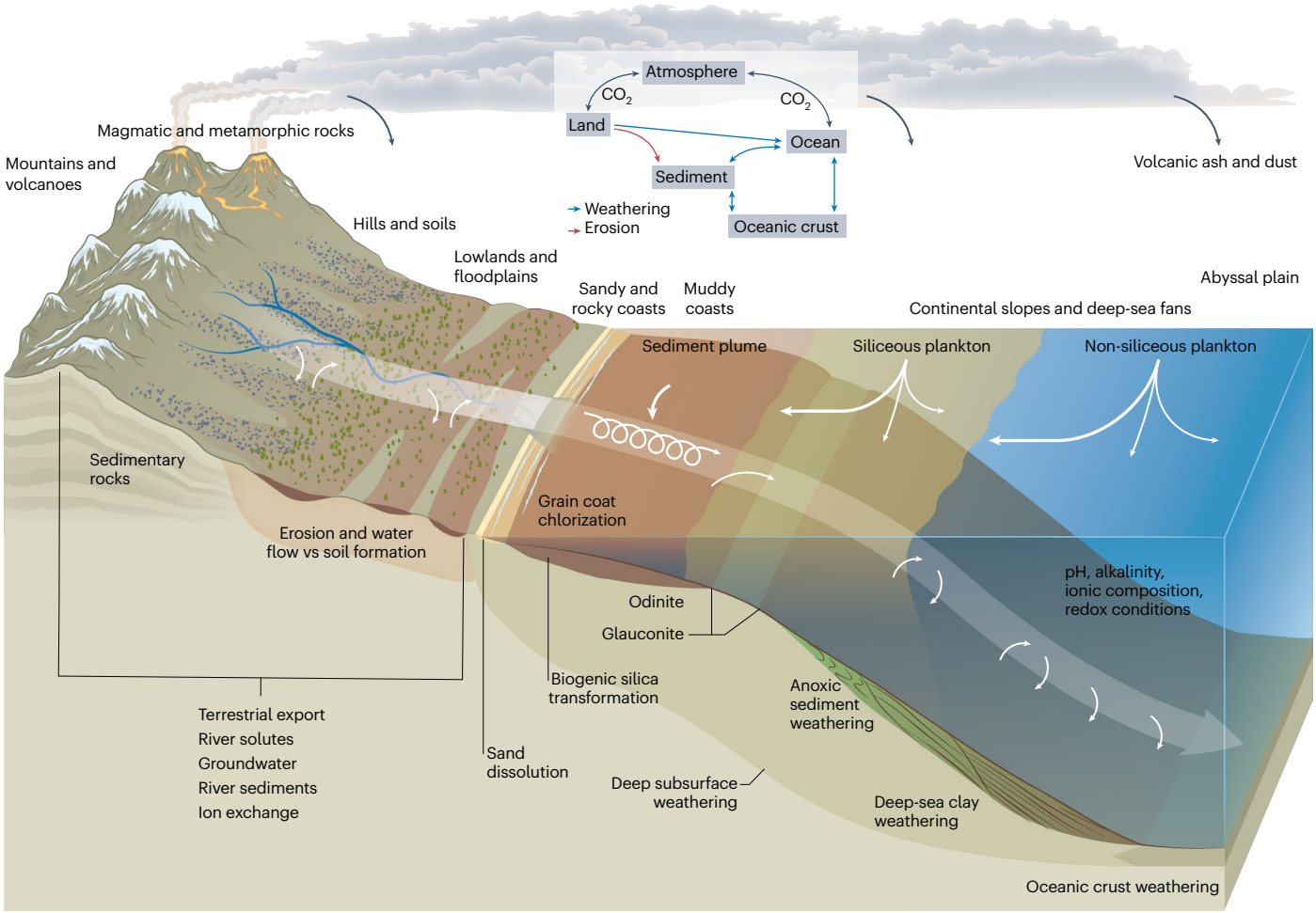

Fig. 1 | Summary of selected weathering environments and processes along Earth's weathering continuum. Corresponding global flux estimates are compiled in Supplementary Fig. 1.

reaction balances increasingly depend on (silicate) reactant composition, non-silicate product suites and their evolution with sediment depth[14,15,18,20,21,50]. For example, many methanic active margin sediments receiving relatively fresh basaltic and volcanogenic materials (mafic minerals, ashes) exhibit forward weathering balances, enhancing sedimentary carbon storage[15,18,19]. Anoxic marine sediments rich in feldspar and terrestrial weathering products rather tend to alkalinity-neutral or reverse weathering balances[13,14,18]. Moreover, many stable and redox-stratified sediments transition between net forward and reverse CSW balances with depth, leading to extensive recycling within the sedimentary column[13]. Biological activity stimulates sediment–water exchange fluxes and weathering rates in these settings[13,17,31]. In dynamic sediments, weathering rates and sediment–water exchange fluxes are promoted by advective flow and physical reworking[1,13,17,30,51].

Thus, W_t/E ratios seem to modulate marine weathering balances directly through effects on silicate composition and indirectly via sediment biogeochemistry. River discharge, oceanic currents and gravity flows eventually transport sediments across and along the shelf or shuttle them down the continental slope into the deep sea[17,52], connecting various marine weathering environments with increasing marine biogenic influence. Interactions between sediments and the underlying oceanic crust and recycling within the sedimentary cover shift net reaction balances and limit the associated alkalinity release to seawater. Given this downstream coupling, Earth's silicate weathering feedback (Box 2) may be governed by the dynamics of a 'weathering continuum', that is, the relative contributions and coupling of various, transport-connected weathering environments from mountains to the deepest sedimentary basins.

Factors governing Earth's silicate weathering continuum

The products, reaction balances, rates and resulting local alkalinity change of CSW (ΔAlk) are governed by reactant mixes (lithology, sediment composition) and environmental boundary conditions (transport regimes, ambient biogeochemistry, temperature; Box 1)[13,17].

Reactant mixes are set by the magmatic, metamorphic and deeper diagenetic processes that form crustal rocks and subsequent chemical and physical processing in a given sequence of weathering environments (Figs. 1 and 2). There is a tendency to forward weathering balances of magmatic and metamorphic rocks and volcanic ashes, which decreases with magmatic differentiation from (ultra-)mafic to felsic rocks (Box 1). Moreover, as forward silicate weathering on land proceeds and removes cations, the resulting changes tend to shift the downstream marine systems towards alkalinity-neutral and reverse CSW (Box 1). Thus, magmatic and tectonic activity should stimulate forward weathering balances through rapid erosion, and sediment dispersal, particularly in (ultra-)mafic volcanic landscapes. In combination with a wet and warm climate and efficient drainage systems, the global alkalinity change of CSW, ΔAlk_{glob}, would be maximized, as in large parts of today's Southeast Asia[8,10,53] (Fig. 2a). At such low W_t/E much of the material would reach the ocean largely unweathered, but fragmented, inheriting a potential for forward marine weathering to the corresponding ocean margins, further increasing ΔAlk_{glob}. In cold dry climates, erosion is expected to dominate over terrestrial weathering[54], eventually facilitating forward terrestrial and marine CSW. Weathering rates may be limited by temperature and water availability on land in

https://doi.org/10.1038/s41561-025-01743-y

BOX 2

Earth's weathering feedback

Most global carbon(–silica) cycle models implement CSW through a phenomenological rate law, directly relating weathering fluxes (W, representing ΔAlk_{glob} and subsequent carbonate burial) to atmospheric pCO_2[5,25]:

$$W = W_{initial}(pCO_2/pCO_{2,initial})^n. \quad (1)$$

$W_{initial}$ is the forward CSW flux balancing the carbon cycle when $pCO_2 = pCO_{2,initial}$, while the exponent n reflects empirical relationships between CO_2, climate, erosion, vegetation and weathering[5,25]. However, changes in feedback functioning must be considered to reconcile the formulation with the palaeo-record[25,89]. Indeed, this formulation accounts for W_t and, perhaps, forward weathering of submarine basalts, but does not consider marine sediment weathering and variable reaction balances explicitly. The incorporation of reverse marine weathering into carbon(–silica) cycle models has advanced our understanding of weathering feedback dynamics and could, perhaps, explain much of the observed variability in Earth's feedback functioning, but it has largely been considered in isolation from terrestrial processes[32,58,59,79,81,83]. To demonstrate how weathering continuum dynamics may affect carbon cycle dynamics, we extend equation (1) with a phenomenological marine CSW term (W_m) that transitions between forward ($\Delta Alk > 0$) and reverse ($\Delta Alk < 0$) weathering on the basis of W_t/E:

$$W = W_t + W_m = W_{t,initial}(CO_2/CO_{2,initial})^n - \left(m\frac{(W_t/E)}{(W_t/E)_{initial}} - m\right). \quad (2)$$

The parameters m and $\frac{(W_t/E)}{(W_t/E)_{initial}}$ ensure that, at initial pCO_2 and W_t/E, net marine weathering is alkalinity neutral[13]. At high $\frac{(W_t/E)}{(W_t/E)_{initial}}$, virtually all material is weathered before erosion and downstream transport, fostering reverse W_m, and vice versa. Observed modern W_t/E ratios range from ~0.03 to 0.09 (ref. 32). Given the complexity of and absence of consensus about the main factors governing marine CSW rates, this formulation implies the simplification that E remains

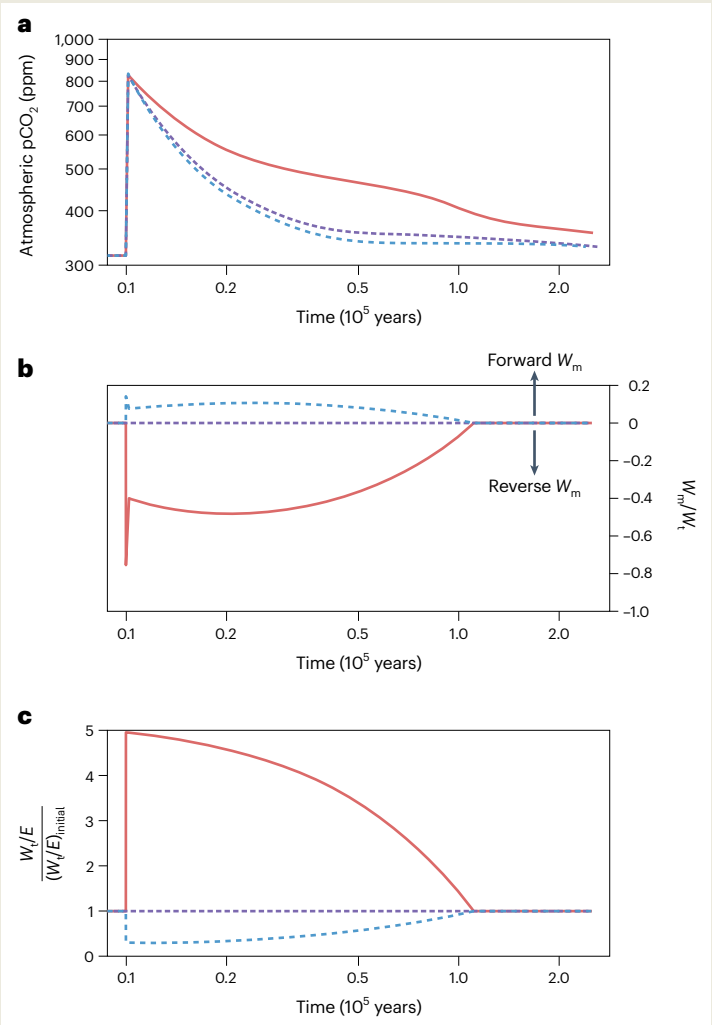

Box Fig. 2 | a–c, Results of a carbon cycle model with a coupled W_t and W_m feedback that is mediated by E. The model was perturbed by a single pulse of carbon dioxide and the recovery in response to three different silicate weathering scenarios is plotted over time (note logarithmic scale). We present a reference scenario with constant W_t/E (purple line), and explore a fivefold increase in W_t/E (~50% increase in reverse W_m, red line, $\Delta Alk < 0$) and a twofold decrease in W_t/E (+20% forwards W_m, blue line, $\Delta Alk > 0$).

(continued from previous page)

high enough to sustain marine sediment CSW and reaction balances govern W_m. Equation (2) was implemented into a modern, otherwise standard carbon cycle model (Supplementary Data 2). This model does not attempt realistic representation of carbon cycling through Earth's history, but allows us to explore first-order effects of the silicate weathering continuum.

We perturbed the system by a pulsed CO_2 injection and imposed the condition that W_t/E either remains constant or immediately decreases or increases coincident with the carbon perturbation to then recover linearly to initial values within 100 kyr (Box Fig. 2c). If W_t/E decreases during the perturbation, forward marine weathering increases (blue, short-dashed line), but if W_t/E increases, marine weathering becomes reverse (red, solid line). Reverse W_m prolongs the system's recovery and elevates post-perturbation pCO_2, while forward W_m accelerates recovery.

these settings, but the sediments would be prone to weathering in the marine realm, particularly at elevated temperatures in the deeper subsurface[21]. The tendency to forward marine CSW can be best expressed at relatively low ambient pH and Si, suppressing reverse components and further increasing ΔAlk_{glob}. Moreover, silica-rich but aluminium–iron-poor conditions can lead to the production of authigenic opal[55,56], promoting the forward weathering component. Rapid and forward marine weathering fluxes are aided by physical and biological factors such as wave action[30] and benthic activity[13,15,31].

In contrast, flat cratons, made up of sedimentary rocks or covered by thick, impermeable soils, such as large parts of today's Amazon and Congo river lowlands, minimize terrestrial weathering fluxes and export cation-depleted, Si–Al–Fe- and metal (oxy-)hydroxide-enriched sediments, prone to reverse weathering in the marine realm (Fig. 2b). These reverse CSW rates may become limited by reactant supply in areas of low continental erosion rates and distal from large rivers. The reverse tendency of marine CSW is maximized by high ambient pH and Si, Al availability and sustained suboxic conditions, as found in dynamic, terrigenous shelf sediments[17]. Thus, high-sea-level periods with submerged extensive shelves would further promote reverse weathering, while low sea level and freshwater-dominated shelves would strengthen the forward CSW component (Fig. 2). In past oceans, ferruginous and siliceous conditions prevailed and have probably promoted an ocean-wide tendency to reverse weathering balances[57,58].

Weathering of oceanic crust has a strong tendency to forward weathering because of its dominantly mafic composition, which is, however, moderated by seawater chemistry (pH, alkalinity, Si concentrations) and offset by silicate and carbonate precipitation and interactions with the detrital and marine biogenic sediment commonly overlying these rocks[18,20,27].

Consequently, the distribution of weathering environments, each with distinct ΔAlk, govern ΔAlk_{glob}, Earth's weatherability and the strength of the weathering feedback in the carbon cycle[24,25]. A strong feedback results in (1) lower atmospheric CO_2 concentrations for a given endogenic degassing rate at steady state and (2) shorter recovery periods after pulsed carbon cycle perturbations in a maximum-ΔAlk_{glob} world (figure in Box 2). While a major component of the global alkalinity and carbon cycles, the Earth's silicate weathering continuum acts in concert with various non-silicate processes to shape Earth system evolution, including organic carbon, nutrient, carbonate and iron sulfide cycling.

Carbon cycle dynamics and shared forcings

CSW is a major global carbon sink, traditionally considered to balance solid Earth CO_2 degassing. However, non-silicate rock and sediment components modulate carbon cycling too, including organic matter, carbonate and (iron) sulfide minerals, which often co-occur in sedimentary rocks. Terrestrial carbonate weathering currently provides ~60–70% of the riverine alkalinity supply[8] and marine weathering of terrigenous carbonates probably adds another ~10% to this flux[59], but their net effects on the carbon cycle are largely compensated by biogenic carbonate burial after ~50–100 kyr[60]. Systematic shifts in carbonate weathering and burial could affect long-term carbon cycling[61,62] and are tied to CSW and respiration in marine sediments[13,19,63]. Moreover, sulfide mineral formation and burial in anoxic sediments provide net preservation of alkalinity generated by dissimilatory sulfate reduction (currently ~20% of riverine alkalinity supply), since this reduced sulfur is not (directly) re-oxidized to produce sulfuric acid[60]. Because terrestrial and marine CSW are involved in nutrient cycling and acid–base chemistry (Box 1), they may enhance or reduce sulfide burial, depending on local CSW balances. In exhumed and subaerially exposed sedimentary rocks and reworked surface sediments, sulfide minerals are oxidized to produce sulfuric acid[6]. If rocks and sediments are weathered by sulfuric instead of carbonic acid, carbonate weathering could become a long-term carbon source and CSW might sequester less carbon. Moreover, oxidation of fossil organic carbon in sedimentary rocks is a direct source of CO_2 to the atmosphere[6], while net burial of organic matter in marine sediments sequesters carbon and provides net preservation of alkalinity generated during nitrate-based photosynthesis[60]. These redox-sensitive processes are also subject to oxygen and temperature feedbacks[24,64]. Burial of organic matter and biominerals eventually couples to CSW through reaction-balance-dependent nutrient cycling and the production of protective clay–organic matter associations in soils and sediments[65].

Oxidative and carbonate weathering in mountains tend to be erosion limited, often accelerating with erosion[6,66], perhaps countering forward shifts of CSW. Moreover, changes in climate and water table can shift the balance between carbonate and sulfide weathering, although signals are often highly convoluted[67]. Burial of reduced components (increasing ocean alkalinity, consuming carbon and nutrients) and authigenic carbonates (consuming alkalinity and carbon) in marine sediments are largely tied to sedimentation dynamics, organic matter diagenesis, metal (oxy-)hydroxide supply and CSW. Burial and CSW rates are highest at the ocean margins and shelves[17,47], so high sea level and extensive, productive shelves promote carbon storage and variable alkalinity fluxes through these processes[17]. Thus, the global cycles of carbonates, silicates, sulfur, iron and organic matter are coupled and share forcings, such as erosion and sedimentation, and vary simultaneously, but in multiple directions and on different, overlapping timescales with environmental and tectonic changes to readjust the carbon cycle[6,7]. The long-term stability of Earth surface conditions suggests that the nature of this covariation is to counter perturbation and minimize fluctuation[68]. Still, the recovery behaviour from perturbations and variability of carbon cycle dynamics remain enigmatic and highlight the complex interplay of various processes that act in concert to shape the Earth system.

Silicate weathering continuum dynamics in Earth's history

Here we briefly review evidence for large-scale changes in the silicate weathering continuum dynamics in a range of selected scenarios from the Earth's history, formulating testable hypotheses and highlighting open questions.

The emergence of continents

Forward, terrestrial CSW and the export of detrital aluminosilicates are expected at the onset of subaerial and freshwater weathering following

https://doi.org/10.1038/s41561-025-01743-y

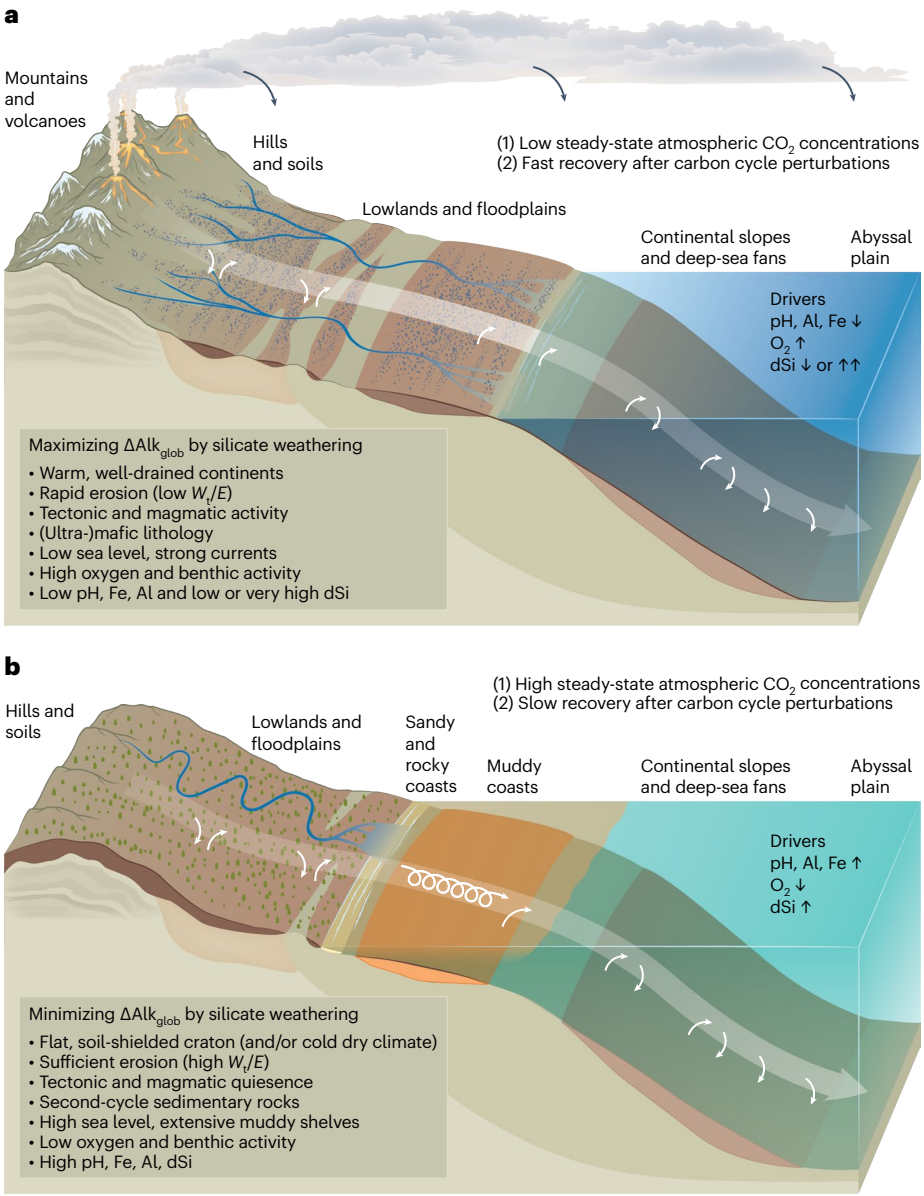

Fig. 2 | Illustration of hypothetical endmember scenarios. a,**b**, Scenarios maximizing (**a**) and minimizing (**b**) CSW-related alkalinity fluxes globally. Drivers of shifts in reaction balances (forwards versus reverse weathering) are indicated.

the growth of granitic continental crust. Indeed, such a change seems to be reflected in a shift from siliceous, ferromagnesian clays (for example, serpentine and talc group) to aluminous clays (for example, kaolinite and beidellite)[69]. Increasing topography and submerged continental shelves would have further diversified the range of weathering environments, reactant distributions and ΔAlk_{glob}. For example, a decline in chert abundance from the Archaean to the Proterozoic[70] suggests fundamental changes in marine silicate authigenesis, perhaps due to reverse weathering of newly introduced detrital aluminosilicates in a silicon-rich ocean. Although quantification of global weathering balances remains difficult, reverse weathering probably contributed to a warm, CO_2-rich and stable climate during the Precambrian[58,71] and may have been counteracted by a global rise in forward CSW on land.

The rise of land plants

The evolution of terrestrial biota and spread of vascular plants across continents has been linked to a long-term, early-to-mid Palaeozoic decline in atmospheric CO_2[72] and to substantial, but complex, changes in hydrology[73,74]. Increasing CSW rates, soil stabilization and water retention within the regolith have probably increased W_t/E and organic carbon burial[72,73,75], with unknown consequences for marine weathering rates and balances. Mass balance constraints[73] and Li-isotope evidence suggest a shift away from large fluxes of reverse weathering towards dominantly continental, forward CSW[76], but the roles of the various weathering environments and interactions with organic carbon cycling in shaping this transition remain elusive.

Permian–Triassic boundary

The end Permian was the most extreme biotic crisis in Earth's history and was probably caused by a massive carbon injection, followed by warming and widespread ocean anoxia[77]. To explain the associated strongly protracted recovery of the Earth system from this crisis, it has been proposed that the weathering feedback (Box 2) was weakened due to the depletion of weatherable cation-rich material in the upper continental crust, allowing extreme temperatures to persist for millions of years[78]. Alternatively, it has been suggested that the loss of a biological SiO_2 factory could have increased ocean Si concentrations, promoting extensive reverse weathering, which may have decreased ΔAlk_{glob} and

protracted the warmth[79]. The weathering continuum hypothesis links these two models, suggesting that high W_t/E may have promoted more reverse marine weathering, driven by the supply of cation–depleted products from terrestrial weathering under rising ambient silicic acid concentrations in the absence of efficient silicification.

Eocene global warming events

The Eocene (56-34 Ma), a period of globally warm temperatures, experienced periodic transient global warming events, marked by massive carbon input into the ocean–atmosphere system. The ocean became more acid, leading to a strong rise in the ocean's calcite compensation depth[80]. During the Palaeocene–Eocene Thermal Maximum (around 56 Ma), warming, intensified hydrological cycling, increased erosion and volcanic ash supply seem to have facilitated the promotion of forward weathering at low W_t/E[37,81,82]. The dissolved silica and nutrients released from this forward weathering overshoot seem to have stimulated productivity and driven chert formation[56], suggesting limited reverse weathering in large parts of the ocean.

In contrast, intense forward weathering during the Middle Eocene Climatic Optimum (~40.5 Ma) appears to have been followed by enhanced soil and clay formation and alkalinity retention, leading to a weakening of Earth's weathering feedback and to protracted warmth[83]. This indicates a shift to increasing reverse weathering in response to high W_t/E, as proposed for the end-Permian mass extinction. However, the locus of clay formation remains debated[83,84] and the links between W_t/E, ecosystem dynamics, marine sediment CSW, carbon cycling and recovery timescales remain to be assessed in detail.

Short timescales

CSW is traditionally considered to occur slowly over million-year timescales[5,24]. However, laboratory and field studies demonstrate that replacement of detrital and biogenic silicates by marine authigenic clays can proceed within days to months when the necessary reactant mixtures are provided[16,85]. Moreover, experiments with tephra and mafic mineral weathering demonstrate that these reactions proceed fast enough to have an impact on human timescales, similar to carbonate and organic matter processes. This makes the amendment of soils and sediments with reactive, cation-rich silicates a potentially viable approach for ocean alkalinization, carbon dioxide reduction and agricultural nutrient supply[86–88]. However, unknown effects on downstream environments of these 'enhanced weathering' techniques influence net alkalinity fluxes and must be considered when quantifying and verifying such methods. Moreover, CSW balances in specific environments may shift rapidly in response to changes in climate, land cover, river transport, sea level and ocean circulation, influencing nutrient and carbon cycling across timescales ranging from seasonal to glacial–interglacial timescales.

Understanding, reconstructing and predicting weathering

Clearly, carbon cycle and Earth system models, as well as environmental assessments and carbon dioxide removal strategies, will benefit from adopting a weathering continuum perspective. A substantial body of work has elucidated terrestrial silicate weathering dynamics at catchment to global scales[8,10,53], resulting in increasingly sophisticated formulations incorporated into global carbon cycle[5,25,89] and Earth system models[23,26]. However, these approaches neglect or oversimplify marine sediment CSW and the variability of reaction balances. Reactant distributions, the sequence of weathering environments, their local reaction–transport dynamics and downstream coupling need to be resolved in a way that is compatible with the demanding computational requirements of an Earth system-scale model to fully represent the silicate weathering continuum. Comparing crustal, detrital, pedogenic and marine authigenic mineral suites with palaeogeographical constraints on the distribution of environments may provide reasonable constraints on regional weathering balances in the past. The isotopic composition of bulk seawater Sr, Os, Be, Li and major cations provides complementary regional and global constraints on the evolution of weathering continuum dynamics throughout Earth's history[32,58,81,83,89,90]. Weathering continuum models will ultimately allow us to assess the relative roles and interactions of silicate weathering continuum dynamics and other carbon cycle processes, such as those related to carbonates, organic matter and iron sulfide, in time and space.

Conclusions

Silicate weathering proceeds in multiple, transport-coupled environments from mountain ranges to the deepest sedimentary basins, with variable weathering rates, reaction balances and carbon cycle impacts, that is, Earth's silicate weathering continuum. This continuum of reaction balances and coupling of environments provide a perspective on the role of silicate weathering in global biogeochemical cycles and its relationship to carbonate, organic and redox processes. Understanding silicate weathering continuum dynamics will help us to better understand how weathering shaped Earth system evolution in concert with life and forces of Earth's interior, and how anthropogenic perturbations affect Earth's future.

Data availability

All data are available as a supplement to the online version of this document or upon request from the corresponding author.

Code availability

All codes are available as a supplement to the online version of this document or upon request from the corresponding author.

References

1. Ruiz-Agudo, E. et al. Control of silicate weathering by interface-coupled dissolution–precipitation processes at the mineral–solution interface. *Geology* **44**, 567–570 (2016).
2. Hellmann, R. et al. Unifying natural and laboratory chemical weathering with interfacial dissolution–reprecipitation: a study based on the nanometer-scale chemistry of fluid–silicate interfaces. *Chem. Geol.* **294/295**, 203–216 (2012).
3. Berner, E. K. & Berner, R. A. *Global Environment: Water, Air, and Geochemical Cycles* (Princeton Univ. Press, 2012).
4. Jeandel, C. & Oelkers, E. H. The influence of terrigenous particulate material dissolution on ocean chemistry and global element cycles. *Chem. Geol.* **395**, 50–66 (2015).
5. Berner, R. A. A model for atmospheric CO_2 over Phanerozoic time. *Am. J. Sci.* **291**, 339–376 (1991).
6. Hilton, R. G. & West, A. J. Mountains, erosion and the carbon cycle. *Nat. Rev. Earth Environ.* **1**, 284–299 (2020).
7. Kemeny, P. C., Torres, M. A., Fischer, W. W. & Blättler, C. L. Balance and imbalance in biogeochemical cycles reflect the operation of closed, exchange, and open sets. *Proc. Natl Acad. Sci. USA* **121**, e2316535121 (2024).
8. Hartmann, J., Moosdorf, N., Lauerwald, R., Hinderer, M. & West, A. J. Global chemical weathering and associated P-release—the role of lithology, temperature and soil properties. *Chem. Geol.* **363**, 145–163 (2014).
9. Mayfield, K. K. et al. Groundwater discharge impacts marine isotope budgets of Li, Mg, Ca, Sr, and Ba. *Nat. Commun.* **12**, 148 (2021).
10. Brantley, S. L., Shaughnessy, A., Lebedeva, M. I. & Balashov, V. N. How temperature-dependent silicate weathering acts as Earth's geological thermostat. *Science* **379**, 382–389 (2023).
11. Ibarra, D. E. et al. Differential weathering of basaltic and granitic catchments from concentration–discharge relationships. *Geochim. Cosmochim. Acta* **190**, 265–293 (2016).

12. Lupker, M. et al. Predominant floodplain over mountain weathering of Himalayan sediments (Ganga basin). *Geochim. Cosmochim. Acta* **84**, 410–432 (2012).
13. Wallmann, K., Geilert, S. & Scholz, F. Chemical alteration of riverine particles in seawater and marine sediments: effects on seawater composition and atmospheric CO_2. *Am. J. Sci.* **323**, 7 (2023).
14. Aloisi, G., Wallmann, K., Drews, M. & Bohrmann, G. Evidence for the submarine weathering of silicate minerals in Black Sea sediments: possible implications for the marine Li and B cycles. *Geochem. Geophys. Geosyst.* **5**, QO4007 (2004).
15. Wallmann, K. et al. Silicate weathering in anoxic marine sediments. *Geochim. Cosmochim. Acta* **72**, 3067–3090 (2008).
16. Michalopoulos, P. & Aller, R. C. Rapid clay mineral formation in Amazon delta sediments: reverse weathering and oceanic elemental cycles. *Science* **270**, 614–617 (1995).
17. Aller, R. C. & Wehrmann, L. in *Treatise on Geochemistry* 3rd end, Vol. 4 (eds Anbar, A. & Weis, D.) 573–629 (2025).
18. Torres, M. E., Milliken, K. L., Hüpers, A., Kim, J. H. & Lee, S. G. Authigenic clays versus carbonate formation as products of marine silicate weathering in the input sequence to the Sumatra subduction zone. *Geochem. Geophys. Geosyst.* **23**, e2022GC010338 (2022).
19. Torres, M. E. et al. Silicate weathering in anoxic marine sediment as a requirement for authigenic carbonate burial. *Earth Sci. Rev.* **200**, 102960 (2020).
20. Aplin, A. C. & Taylor, K. G. in *Environmental Mineralogy II* (eds Vaughan, D. & Wogelius, R. A.) Vol. 13, 123–175 (Mineralogical Society of Great Britain and Ireland, 2013).
21. Milliken, K. L. in *Treatise on Geochemistry* Vol. 7 (eds Holland, H. D. & Turekian, K. K.) 159–190 (Pergamon, 2003).
22. Müller, G. Diagenesis in argillaceous sediments. *Dev. Sedimentol.* **8**, 127–177 (1967).
23. Park, Y. et al. Emergence of the Southeast Asian islands as a driver for Neogene cooling. *Proc. Natl Acad. Sci. USA* **117**, 25319–25326 (2020).
24. Isson, T. T. et al. Evolution of the global carbon cycle and climate regulation on Earth. *Glob. Biogeochem. Cycles* **34**, e2018GB006061 (2020).
25. Penman, D. E., Caves Rugenstein, J. K., Ibarra, D. E. & Winnick, M. J. Silicate weathering as a feedback and forcing in Earth's climate and carbon cycle. *Earth Sci. Rev.* **209**, 103298 (2020).
26. Mills, B. J. W., Donnadieu, Y. & Goddéris, Y. Spatial continuous integration of Phanerozoic global biogeochemistry and climate. *Gondwana Res.* **100**, 73–86 (2021).
27. Coogan, L. A. & Gillis, K. M. Low-temperature alteration of the seafloor: impacts on ocean chemistry. *Annu. Rev. Earth Planet. Sci.* **46**, 21–45 (2018).
28. Luttge, A., Arvidson, R. S., Fischer, C. & Kurganskaya, I. Kinetic concepts for quantitative prediction of fluid–solid interactions. *Chem. Geol.* **504**, 216–235 (2019).
29. Müller, G., Fritzsche, M. B. K., Dohmen, L. & Geisler, T. Feedbacks and non-linearity of silicate glass alteration in hyperalkaline solution studied by in operando fluid-cell Raman spectroscopy. *Geochim. Cosmochim. Acta* **329**, 1–21 (2022).
30. Fabre, S., Jeandel, C., Zambardi, T., Roustan, M. & Almar, R. An overlooked silica source of the modern oceans: are sandy beaches the key? *Front Earth Sci.* **7**, 231 (2019).
31. Meysman, F. J. R. & Montserrat, F. Negative CO_2 emissions via enhanced silicate weathering in coastal environments. *Biol. Lett.* **13**, 20160905 (2017).
32. Caves Rugenstein, J. K., Ibarra, D. E. & von Blanckenburg, F. Neogene cooling driven by land surface reactivity rather than increased weathering fluxes. *Nature* **571**, 99–102 (2019).
33. Mackenzie, F. T. & Garrels, R. M. Chemical mass balance between rivers and oceans. *Am. J. Sci.* **264**, 507–525 (1966).
34. West, A. J., Galy, A. & Bickle, M. Tectonic and climatic controls on silicate weathering. *Earth Planet. Sci. Lett.* **235**, 211–228 (2005).
35. Thorpe, M. T., Hurowitz, J. A. & Dehouck, E. Sediment geochemistry and mineralogy from a glacial terrain river system in southwest Iceland. *Geochim. Cosmochim. Acta* **263**, 140–166 (2019).
36. Müller, G., Middelburg, J. J. & Sluijs, A. Introducing GloRiSe—a global database on river sediment composition. *Earth Syst. Sci. Data* **13**, 3565–3575 (2021).
37. Longman, J. et al. Marine diagenesis of tephra aided the Palaeocene–Eocene Thermal Maximum termination. *Earth Planet. Sci. Lett.* **571**, 117101 (2021).
38. Beckingham, L. E. et al. Evaluation of accessible mineral surface areas for improved prediction of mineral reaction rates in porous media. *Geochim. Cosmochim. Acta* **205**, 31–49 (2017).
39. Winnick, M. J. & Maher, K. Relationships between CO_2, thermodynamic limits on silicate weathering, and the strength of the silicate weathering feedback. *Earth Planet. Sci. Lett.* **485**, 111–120 (2018).
40. Bouchez, J. et al. Floodplains of large rivers: weathering reactors or simple silos? *Chem. Geol.* **332/333**, 166–184 (2012).
41. Swindale, L. D. & Fan, P. F. Transformation of gibbsite to chlorite in ocean bottom sediments. *Science* **157**, 799–800 (1967).
42. Journet, E., Balkanski, Y. & Harrison, S. P. A new data set of soil mineralogy for dust-cycle modeling. *Atmos. Chem. Phys.* **14**, 3801–3816 (2014).
43. Hayes, M. O. Relationships between coastal climate and bottom sediment type on the inner continental shelf. *Mar. Geol.* **5**, 111–132 (1967).
44. Ku, T. C. W. & Walter, L. M. Syndepositional formation of Fe-rich clays in tropical shelf sediments, San Blas Archipelago, Panama. *Chem. Geol.* **197**, 197–213 (2003).
45. Rahman, S., Aller, R. C. & Cochran, J. K. The missing silica sink—revisiting the marine sedimentary Si cycle using cosmogenic ^{32}Si. *Glob. Biogeochem. Cycles* **31**, 1559–1578 (2017).
46. Petzing, J. & Chester, R. Authigenic marine zeolites and their relationship to global volcanism. *Mar. Geol.* **29**, 253–271 (1979).
47. Berner, R. A. A new geochemical classification of sedimentary environments. *J. Sediment. Res.* **51**, 359–365 (1981).
48. Aller, R. C., Blair, N. E., Xia, Q. & Rude, P. D. Remineralization rates, recycling, and storage of carbon in Amazon shelf sediments. *Cont. Shelf Res.* **16**, 753–786 (1996).
49. Bao, R. et al. Influence of hydrodynamic processes on the fate of sedimentary organic matter on continental margins. *Glob. Biogeochem. Cycles* **32**, 1420–1432 (2018).
50. Scholz, F., Hensen, C., Schmidt, M. & Geersen, J. Submarine weathering of silicate minerals and the extent of pore water freshening at active continental margins. *Geochim. Cosmochim. Acta* **100**, 200–216 (2013).
51. Michalopoulos, P. & Aller, R. C. Early diagenesis of biogenic silica in the Amazon delta: alteration, authigenic clay formation, and storage. *Geochim. Cosmochim. Acta* **68**, 1061–1085 (2004).
52. Syvitski, J. P. M., Smith, J. N., Calabrese, E. A. & Boudreau, B. P. Basin sedimentation and the growth of prograding deltas. *J. Geophys. Res.* **93**, 6895–6908 (1988).
53. Maher, K. & Chamberlain, C. P. Hydrologic regulation of chemical weathering and the geologic carbon cycle. *Science* **343**, 1502–1504 (2014).
54. Kump, L. R. & Alley, R. B. in *Material Fluxes on the Surface of the Earth* 46–60 (National Research Council, 1994).

55. Riech, V. & von Rad, U. Silica diagenesis in the Atlantic Ocean: diagenetic potential and transformations. In *Deep Drilling Results in the Atlantic Ocean: Continental Margins and Paleoenvironment* (eds Talwani, M. et al.) 315–340 (American Geophysical Union, 1979).
56. Penman, D. E., Keller, A., D'haenens, S., Kirtland Turner, S. & Hull, P. M. Atlantic deep-sea cherts associated with Eocene hyperthermal events. *Paleoceanogr. Paleoclimatol.* **34**, 287–299 (2019).
57. Tosca, N. J., Guggenheim, S. & Pufahl, P. K. An authigenic origin for Precambrian greenalite: implications for iron formation and the chemistry of ancient seawater. *Bull. Geol. Soc. Am.* **128**, 511–530 (2016).
58. Isson, T. T. & Planavsky, N. J. Reverse weathering as a long-term stabilizer of marine pH and planetary climate. *Nature* **560**, 471–474 (2018).
59. Müller, G., Börker, J., Sluijs, A. & Middelburg, J. J. Detrital carbonate minerals in Earth's element cycles. *Glob. Biogeochem. Cycles* **36**, e2021GB007231 (2022).
60. Middelburg, J. J., Soetaert, K. & Hagens, M. Ocean alkalinity, buffering and biogeochemical processes. *Rev. Geophys.* **58**, e2019RG000681 (2020).
61. Derry, L. A. Carbonate weathering, CO_2 redistribution, and Neogene CCD and pCO_2 evolution. *Earth Planet. Sci. Lett.* **597**, 117801 (2022).
62. Boudreau, B. P., Middelburg, J. J. & Luo, Y. The role of calcification in carbonate compensation. *Nat. Geosci.* **11**, 894–900 (2018).
63. Milliken, K. L. & Land, L. The origin and fate of silt sized carbonate in subsurface miocene oligocene mudstones. *Sedimentology* **40**, 107–124 (1993).
64. Maffre, P., Swanson-Hysell, N. L. & Goddéris, Y. Limited carbon cycle response to increased sulfide weathering due to oxygen feedback. *Geophys. Res. Lett.* **48**, e2021GL094589 (2021).
65. Hemingway, J. D. et al. Mineral protection regulates long-term global preservation of natural organic carbon. *Nature* **570**, 228–231 (2019).
66. Bufe, A., Rugenstein, J. K. C. & Hovius, N. CO_2 drawdown from weathering is maximized at moderate erosion rates. *Science* **383**, 1075–1080 (2024).
67. Stolze, L. et al. Climate forcing controls on carbon terrestrial fluxes during shale weathering. *Proc. Natl Acad. Sci. USA* **121**, e2400230121 (2024).
68. Berner, R. A. & Caldeira, K. The need for mass balance and feedback in the geochemical carbon cycle. *Geology* **25**, 955–956 (1997).
69. Hazen, R. M. et al. Clay mineral evolution. *Am. Mineral.* **98**, 2007–2029 (2013).
70. Maliva, R. G., Knoll, A. H. & Simonson, B. M. Secular change in the Precambrian silica cycle: insights from chert petrology. *Bull. Geol. Soc. Am.* **117**, 835–845 (2005).
71. Krissansen-Totton, J. & Catling, D. C. A coupled carbon–silicon cycle model over Earth history: reverse weathering as a possible explanation of a warm mid-Proterozoic climate. *Earth Planet. Sci. Lett.* **537**, 116181 (2020).
72. Berner, R. A. Weathering, plants, and the long-term carbon cycle. *Geochim. Cosmochim. Acta* **56**, 3225–3231 (1992).
73. Ibarra, D. E. et al. Modeling the consequences of land plant evolution on silicate weathering. *Am. J. Sci.* **319**, 1–43 (2019).
74. Seeley, J. T. & Wordsworth, R. D. Episodic deluges in simulated hothouse climates. *Nature* **599**, 74–79 (2021).
75. McMahon, W. J. & Davies, N. S. Evolution of alluvial mudrock forced by early land plants. *Science* **359**, 1022–1024 (2018).
76. Kalderon-Asael, B. et al. A lithium-isotope perspective on the evolution of carbon and silicon cycles. *Nature* **595**, 394–398 (2021).
77. Cui, Y. & Kump, L. R. Global warming and the end-Permian extinction event: proxy and modeling perspectives. *Earth Sci. Rev.* **149**, 5–22 (2015).
78. Kump, L. R. Prolonged Late Permian–Early Triassic hyperthermal: failure of climate regulation? *Philos. Trans. R. Soc. A* **376**, 20170078 (2018).
79. Isson, T. T. et al. Marine siliceous ecosystem decline led to sustained anomalous Early Triassic warmth. *Nat. Commun.* **13**, 3509 (2022).
80. Zachos, J. C. et al. Rapid acidification of the ocean during the Paleocene–Eocene Thermal Maximum. *Science* **308**, 1611–1615 (2005).
81. Pogge von Strandmann, P. A. E. et al. Lithium isotope evidence for enhanced weathering and erosion during the Paleocene–Eocene Thermal Maximum. *Sci. Adv.* **7**, eabh4224 (2021).
82. Carmichael, M. J. et al. Hydrological and associated biogeochemical consequences of rapid global warming during the Paleocene–Eocene Thermal Maximum. *Glob. Planet. Change* **157**, 114–138 (2017).
83. Krause, A. J., Sluijs, A., van der Ploeg, R., Lenton, T. M. & Pogge von Strandmann, P. A. E. Enhanced clay formation key in sustaining the Middle Eocene Climatic Optimum. *Nat. Geosci.* **16**, 730–738 (2023).
84. Banerjee, S., Choudhury, T. R., Saraswati, P. K. & Khanolkar, S. The formation of authigenic deposits during Paleogene warm climatic intervals: a review. *J. Palaeogeogr.* **9**, 27 (2020).
85. Geilert, S. et al. Coastal El Niño triggers rapid marine silicate alteration on the seafloor. *Nat. Commun.* **14**, 1676 (2023).
86. Hartmann, J. et al. Enhanced chemical weathering as a geoengineering strategy to reduce atmospheric carbon dioxide, supply nutrients, and mitigate ocean acidification. *Rev. Geophys.* **51**, 113–149 (2013).
87. Schuiling, R. D. & Krijgsman, P. Enhanced weathering: an effective and cheap tool to sequester CO_2. *Clim. Change* **74**, 349–354 (2006).
88. Longman, J., Palmer, M. R. & Gernon, T. M. Viability of greenhouse gas removal via artificial addition of volcanic ash to the ocean. *Anthropocene* **32**, 100264 (2020).
89. Caves, J. K., Jost, A. B., Lau, K. V. & Maher, K. Cenozoic carbon cycle imbalances and a variable weathering feedback. *Earth Planet. Sci. Lett.* **450**, 152–163 (2016).
90. Dunlea, A. G., Murray, R. W., Santiago Ramos, D. P. & Higgins, J. A. Cenozoic global cooling and increased seawater Mg/Ca via reduced reverse weathering. *Nat. Commun.* **8**, 844 (2017).

Acknowledgements

We thank A. Exel and M. Mullen-Pouw (both Utrecht University) for helping with workshop organization, and thank T. Markus (Utrecht University) for his patience and skill while illustrating Earth's silicate weathering continuum. This work was carried out under the umbrella of the Netherlands Earth System Science Center (NESSC) and supported by an NESSC workshop grant. The project has received funding from the European Union Horizon 2020 research and innovation programme under Marie Skłodowska-Curie grant agreement 847504. D.J.C. and A.S. thank the European Research Council (ERC) under the European Union's Horizon 2020 Research and Innovation Programme for grants 833454 and 771497, respectively. D.J.C. also received a grant from the Knut and Alice Wallenberg Foundation. D.J.J.v.H. acknowledges NWO-Vici grant 865.17.001. J.C.R. received funding from the Colorado State University Warner College Dean's Transdisciplinary Travel Grant. N.J.P. acknowledges support from NASA ICAR Alternative Earths grant. A.N.-S. received funding from NSF grant numbers EAR-1554502 and EAR-2012730. W.-L.H. acknowledges funding from the European Research Council (ERC) under the Consolidator Grant (Project 101087884—MadSilica), Ragnar

Söderbergs stiftelse (project 1/22-A) and STINT (Swedish Foundation for International Cooperation in Research and Higher Education) (project MG2022-9391).

Author contributions

G.T.-M. organized and conceptualized the workshop resulting in this article with the help of J.J.M., A.S. and S.G. All authors helped in conceptualizing the article and figures. G.T.-M. drafted the Abstract, The silicate weathering continuum, Carbon cycle dynamics and shared forcings, Conclusions and Box 1 with inputs from all authors. G.T.-M., C.J. and J.J.M. wrote the introductory section. S.G., A.S. and G.T.-M. wrote Short timescales with inputs from G.-J.R. J.C.R. and G.T.-M. wrote Box 2 and The rise of land plants. J.L., G.T.-M. and A.S. wrote Eocene global warming events. P.R.D.M. and G.T.-M. wrote The emergence of continents with edits from D.J.J.v.H. N.J.P. and G.T.-M. wrote Permian–Triassic boundary. G.T.-M., K.L.M., J.L., W.-L.H., X.Y.Z., D.J.J.v.H., M.H. and J.J.M. contributed particularly to Understanding, reconstructing and predicting weathering. J.C.R. coded the carbon cycle model with inputs from G.T.-M. and N.J.P. G.T.-M. and J.J.M. edited the manuscript. All authors helped in reviewing and improving the manuscript.

Competing interests

The authors declare no competing interests.

Additional information

Supplementary information The online version contains supplementary material available at https://doi.org/10.1038/s41561-025-01743-y.

Correspondence should be addressed to Gerrit Trapp-Müller.

Peer review information *Nature Geoscience* thanks Shouye Yang and the other, anonymous, reviewer(s) for their contribution to the peer review of this work. Primary Handling Editor: Tamara Goldin, in collaboration with the *Nature Geoscience* team.